A SHEAR TRANSFER MODEL FOR ROUGH JOINTS BASED ON CONTACT AND FRACTURE MECHANICS

MARCO PAGGI, ALBERTO CARPINTERI

Politecnico di Torino
Department of Structural, Geotechnical and Building Engineering
Corso Duca degli Abruzzi 24, 10129 Torino, Italy
e-mail: marco.paggi@polito.it, http://staff.polito.it/marco.paggi

Key words: Rough joints, Contact mechanics, Fracture mechanics, Fractality, Size-scale effects

Abstract: This article addresses the fundamental issue of shear transfer across rough joints, a problem of paramount importance in several civil engineering applications. Starting from the examination of the experimental results obtained from shear tests on concrete-concrete joints, rock-rock joints and concrete-soil interfaces, the main features of the physical phenomenon are presented. The experimental results are then interpreted according to a novel formulation based on the integration of contact mechanics, suitable for the description of the pre-peak response of the joint, and nonlinear fracture mechanics, for the description of the post-peak softening branch. The proposed treatment fully takes into account the size-scale effects on the shear response of the joints due to interface roughness, providing a significant step forward with respect to the state-of-the-art modelling based on elasto-plasticity with a history dependent friction coefficient.

1 INTRODUCTION

The treatment of shear transfer across rough joints arises in several civil engineering problems. They range from retrofitting of damaged concrete structures with new concrete overlays [1] or with fiber-reinforced polymers [2] to the analysis of the shear response of rock joints [3] and concrete-soil interfaces in pile foundations [4]. Moreover, it is an aspect of paramount importance for the fundamental understanding of the behaviour of rough interfaces subjected to Mode II deformation. In these problems, although the joint is not glued or soldered as in composites, roughness induces similar effects, as we will quantitatively show in the sequel.

Starting from the experimental evidence, shear tests on rock joints [3], concrete-soil interfaces [4], concrete-concrete cold joints [5] and bolt-fastened concrete layers [1] present common features and show that several mechanisms contribute to shear transfer. The most important are friction, cohesion due to asperity interlocking and the dowel action in the presence of bolts. The shear strength, which is as the peak shear traction evaluated from a shear test, is an increasing function of the normal pressure. This trend is shown in Fig. 1 for shear tests on concrete-soil interfaces [4], where the shear traction q is plotted vs. the sliding displacement g_T.

The amplitude of roughness is also increasing the shear resistance of the joint, as experimentally observed in [3].

The specimen size, on the other hand, leads to an opposite trend, which is difficult to be explained according to classical Euclidean geometry. Large specimens have a lower strength than the small ones [3], as shown in Fig. 2. This size-scale effect on the shear strength has been interpreted in [6-8] by

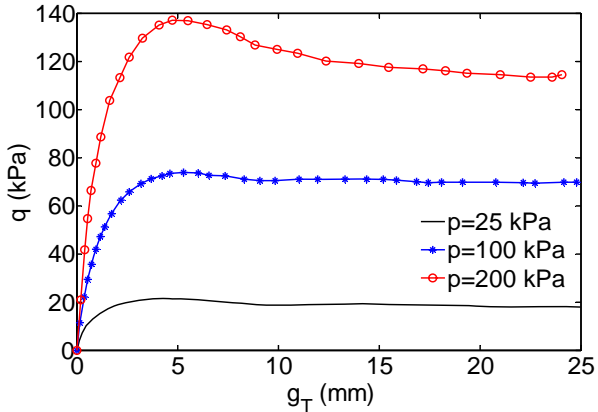considering the fractality of rough contact interfaces.

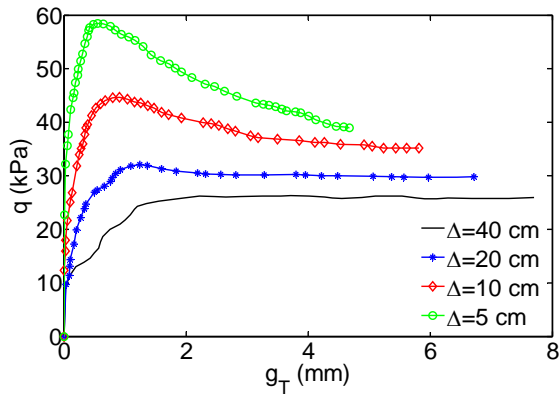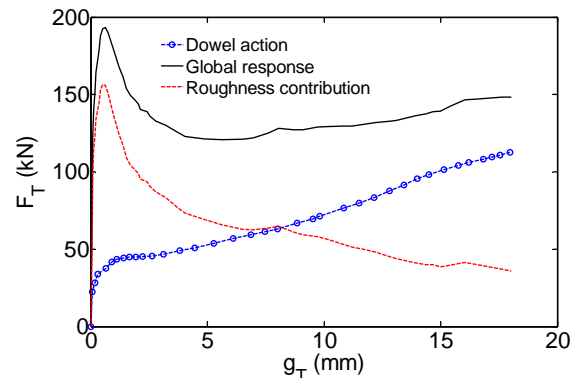**Figure 1**: Shear test results for concrete-soil contact [4] showing the effect of the normal pressure p.

Figure 2: Shear test results for rock-rock contact [3] showing the effect of the specimen size Δ.

The post-peak branch of the curve obtained from a shear test is also very complex and may present a transition from softening –for small specimen sizes or for high normal pressure– to a plastic plateau –for large specimens or for low normal pressure–, see Figs. 1 and 2.

When steel bolts are included, the post-peak branch usually presents hardening. This phenomenon has been investigated in [1] by performing shear tests on concrete-concrete joints fastened using 2 12 steel bolts, for different amplitudes of roughness. The non planarity of the interface is originated by surface blasting with high pressure water (Fig. 3(a)), or with sand (Fig. 3(b)). In both cases, the total tangential force, F_T, is an increasing function of the sliding displacement g_T up to a peak value (thick solid curves in Fig. 3). Afterwards, a softening branch takes place, which is followed by hardening for very large sliding displacements. The dowel action exerted by bolts was also measured in [1] and it is superimposed to the previous figures using a dashed-dotted line. The difference between the curve corresponding to the global response and the curve related to the dowel action is numerically computed here and it represents the shear contribution due to roughness (see the dashed curves in Fig. 3). This contribution shows a softening branch, in close analogy with the previous results displayed in Figs. 1 and 2. Sand blasting induces a roughness amplitude lower than high pressure water blasting and therefore the peak shear strength is lower in Fig. 3(b) than in Fig. 3(a). This confirms that roughness has a decisive role on the frictional response of cold joints.

(a) High pressure water blasted surfaces.
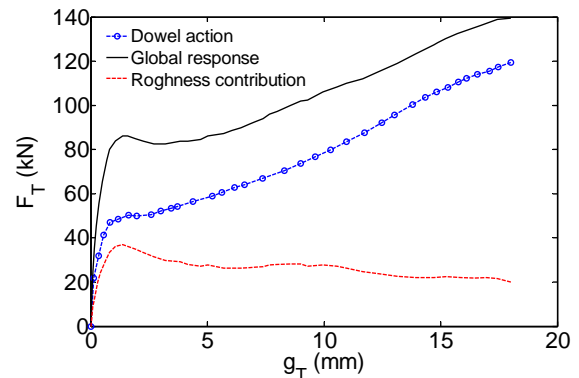
(b) Sand blasted surfaces.

Figure 3: Shear test results for concrete-concrete contact [1] showing the effect of the dowel action and of roughness, for two different surface treatments.

As regards modelling, an attempt to interpret these shear phenomena has been made in the framework of the finite element method and elasto-plasticity. A history dependent friction coefficient according to a semi-empirical expression and fitted on experimental results was proposed in [1] to capture the pre- and post-peak branches of the curves in Fig. 1. Although successful for these tests, the use of seven parameters reduces the possibility to generalize the results of this approach to other types of joints. In fact, all the model parameters are just best-fitting coefficients not related to measurable roughness properties.

In the present contribution, a new model based on the integration of contact mechanics and fracture mechanics is proposed. The novelty of the approach consists in modelling the pre-peak and the post-peak branches of the shear response by using and integrating two different methodologies, a modelling strategy not yet explored in the literature. The nonlinear pre-peak response is considered as the result of the phenomenon of micro-slipping of the asperities in contact. This problem is solved using the contact mechanics approach for rough surfaces proposed in [9] and generalized in [10] for cyclic loading. After achieving the peak shear stress, the post-peak regime is considered to be the result of a phenomenon of cohesion exerted by asperity interlocking. This stage will be modelled by introducing a new Mode II cohesive zone model. The micromechanical contact formulation and the nonlinear fracture mechanics model are integrated to provide a complete description of the joint behaviour. In case of bolt-fastened concrete blocks, the dowel action can also by added to the previous contributions to simulate the post-peak hardening, following the methodology presented in [1].

The main achievement of the proposed model is the ability to take into account the size-scale effect observed in experiments. Moreover, it involves parameters solely dependent on the topology of rough surfaces that can be measured according to tribology standards [11].

2 MODELLING THE PRE-PEAK RESPONSE BY USING CONTACT MECHANICS

3.1 The normal contact problem

Dimensional analysis considerations and incomplete similarity arguments presented in [12] have demonstrated that the normal contact stiffness of a rough joint is a power-law function of the normal pressure. Experimental results and numerical simulations have also confirmed this power-law trend, see [12]. This is due to the non Euclidean (fractal) character of roughness. In dimensionless form, the power-law relation between pressure and mean plane separation is:

$$\frac{\mathrm{d}\tilde{p}}{\mathrm{d}\tilde{d}} \propto \tilde{p}^{\beta} \qquad (1)$$

where the dimensionless variables $\tilde{p} = p\Delta / (E\sigma)$ and $\tilde{d} = d / \sigma$ have been introduced. The variable d is schematically shown in Fig. 4 and represents the distance between the average plane of the composite topography and a rigid flat indenting plane. The variable Δ denotes the upper cut-off length to the power-law behaviour of the power spectral density function of the rough fractal surface [11]. In the present case, it can be related to the lateral size of the sample. The remaining parameters, E and σ, are the Young's modulus and the r.m.s. roughness of the surface.
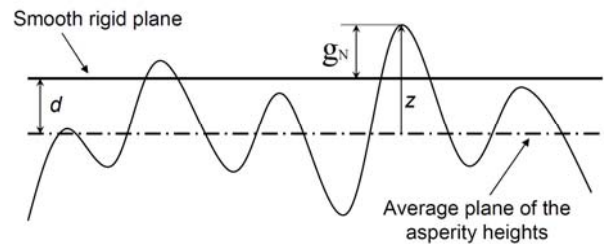

Figure 4: Sketch of the normal contact problem between a equivalent composite rough surface and a smooth rigid plane.

Integration of the ordinary differential equation (1) relating the normal stiffness to the pressure gives the pressure-separation relation.

This relation is exponential only in case of $\beta = 1$ [12]. For the most general case $\beta \neq 1$, we have:

$$\tilde{p} = K(A - B\tilde{d})^{\gamma} \qquad (2)$$

which is a power-law if and only if $A=0$. The exponent γ is related to β via $\gamma = 1/(1-\beta)$. The coefficient K is a scaling factor taking into account the nonlinear size-scale effect on the shear strength. A qualitative sketch of Eq. (2) is shown in Fig. 5. Considering a loading scenario where two rough surfaces are progressively brought into contact from a very large separation, the pressure is increasing by reducing $\tilde{d}$, up to a final configuration denoted by the index f in Fig. 5.
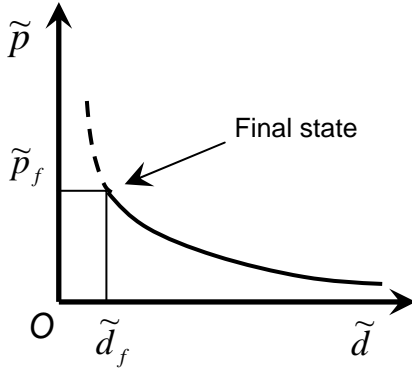

Figure 5: Dimensionless pressure-separation relation.

3.2 The tangential contact problem

Following the approach in [9,10], the solution of the tangential contact problem between rough surfaces can be derived from the solution of the normal contact problem. In formulae we have:

$$\tilde{g}_T = \mu(\tilde{g}_{N,f} - \tilde{g}_N)$$
$$\tilde{q} = \mu(\tilde{p}_f - \tilde{p}) \qquad (3)$$

where μ is the fiction coefficient, $\tilde{g}_T = g_T / \sigma$ is the dimensionless sliding displacement and $\tilde{q} = q\Delta / (E\sigma)$ is the dimensionless tangential traction. Hence, the slip and the tangential tractions can be obtained from the solution of the normal contact problem at the final state of a normal

contact simulation, minus a corrective term related to a lower pressure level.

Equation (3) is sets up in terms of the dimensionless contact compliance, $\tilde{g}_N = g_N / \sigma$, which should be measured from the first point in contact (see Fig. 4). Although a tallest asperity always exists in numerical realization of rough surfaces, its elevation is affected by large variations governed by the extreme value theory. Hence, it is preferable to rewrite Eq. (3) in terms of the mean plane separation, a quantity much more stable from the statistical point of view. Noting that $\tilde{g}_N = \tilde{d}_{max} - \tilde{d}$ and introducing this relation into Eq. (3), we obtain:

$$\tilde{g}_T = \mu(\tilde{d} - \tilde{d}_f)$$
$$\tilde{q} = \mu(\tilde{p}_f - \tilde{p}) \qquad (4)$$

Note that Eq. (4) does not depend on $\tilde{d}_{max}$. The pressure range that can be explored is from 0 up to $\tilde{p}_f$. Correspondingly, the tangential tractions vary from $\tilde{q}_f = \mu\tilde{p}_f$ down to 0. Intermediate values of tractions between 0 and the value corresponding to full slip, $\tilde{q}_f$, will be denoted as $\tilde{q}$. The obtained dimensionless tangential traction vs. sliding relation is qualitatively shown in Fig. 6. It can be considered as a regularization of the Mohr-Coulomb friction law, which would imply zero sliding until full slip takes place for $\tilde{q} = \tilde{q}_f$. This sharp situation would happen only in the limit case of two ideally flat planes in contact. Physically speaking, the reason for this regularization is due to the non constant normal contact pressures supported by the asperities and induced by roughness.

Using Eq. (2), the following explicit relation between $\tilde{q}$ and $\tilde{g}_T$ is obtained:

$$\tilde{q} = \mu\left[\tilde{p}_f - \left(KA - \frac{KB}{\mu}\tilde{g}_T - KB\tilde{d}_f \right)^{\gamma} \right] \qquad (5)$$
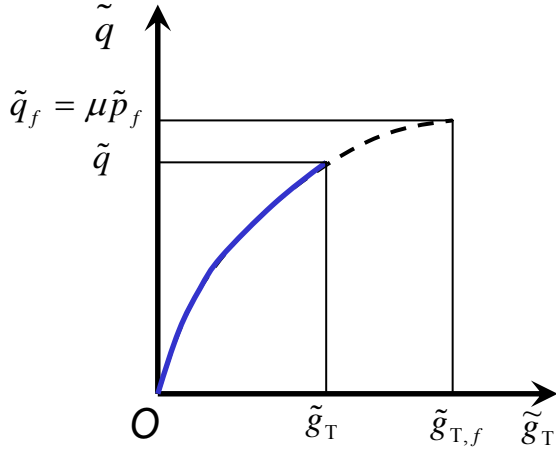
Figure 6: Dimensionless tangential traction-sliding relation.

Figure 7: Tangential traction vs. sliding displacement: numerical predictions (solid lines) and experimental curves (dashed lines).

3.4 Interpretation of the pre-peak experimental results

In this subsection, the experimental shear tests related to the curves in Fig. 2 are numerically simulated and the predicted pre-peak branches are compared with the experimental ones. To do so, the Young's modulus and the r.m.s. roughness are chosen as to represent the rock material analyzed in [3]. The parameters A and B in Eq. (2) are set equal to 2.04 and 0.41, respectively. Four different values of the specimen size, $\Delta = 5$ cm, 10 cm, 20 cm and 40 cm, are considered. The range of dimensionless separations explored is from 5 (large separations, very weak interaction) to 0 (high pressure level). This is also the final state for the application of Eq. (3) and it leads to normal pressure levels consistent with the experimental ones in [3]. Considering K=1, the solid curve in Fig. 7 corresponding to $\Delta = 5$ cm is obtained. All the other curves corresponding to different specimen sizes are obtained by selecting a different Δ in the fomulae and applying the coefficient K reported in Tab. 1.
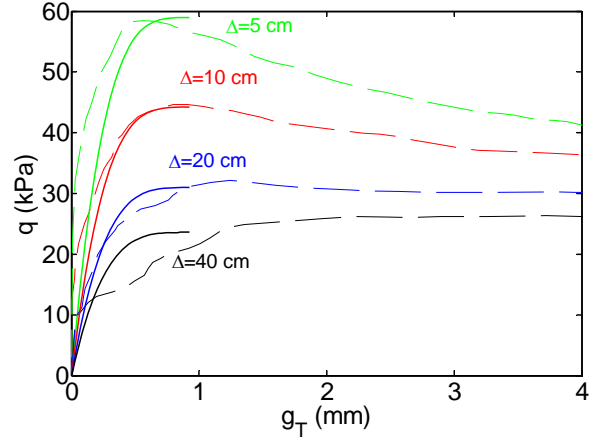
Table 1: Value of the coefficient K in Eq. (2).

Δ (cm)	K
0.05	1.0
0.10	1.5
0.20	2.1
0.40	3.2

It is remarkable to note that, without the use of the coefficient K, the size-scale effect predicted by the application of Eq. (5) would be much higher. The coefficient K re-scales the vertical coordinates and it is related to the size-scale effect on the shear strength of the joint. Hence, the knowledge of this scaling law allows an easy computation of the parameter K by matching the peak traction given by Eq. (5) with K=1 and the shear strength given by the scaling law.

For rocks, the expression of the scaling law for the shear strength has been determined in [7,8] by considering a wide range of length scales ranging from the size of typical laboratory specimens to the size of a natural fault, obtaining $q = q^* \Delta^{-d_q}$. Determining q^* and d_q from best-fitting of experimental results, in logarithmic form we have:

$$\log_{10} q = 4.33 - 0.34 \log_{10} \Delta \qquad (6)$$

Equation (6) fits very well the shear strength results of the tests in Fig. 2, as shown in the comparison of Fig. 8.
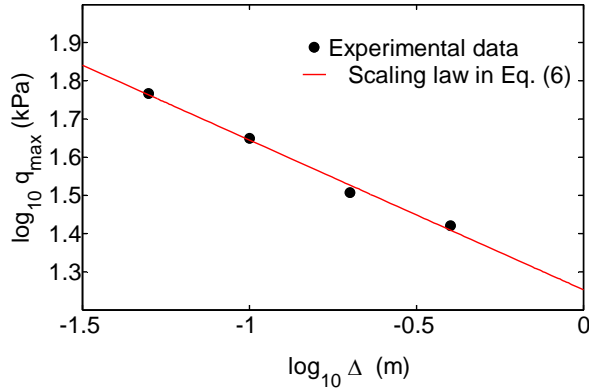

Figure 8: Size-scale effects on the shear strength: experimental data from Fig. 2 vs. scaling law in Eq. (6).

4 MODELLING THE POST-PEAK RESPONSE BY USING FRACTURE MECHANICS

The post-peak branches of the curves in Fig. 2 are modelled in this section according to a cohesive zone approach for Mode II deformation. The cohesion resistance to sliding is due to interlocking between the asperities, an aspect that takes place for large sliding displacements after the achievement of the peak strength. For this analysis, we follow the methodology proposed in [13,14] already adopted for the interpretation of uniaxial tensile tests and compression tests (Mode I problems).

As a preliminary operation, the inelastic contribution to the deformation in the post-peak branch is isolated by removing from the total sliding displacement the elastic deformation of the pre-peak branch. After this operation, the post-peak inelastic traction vs. sliding curves of Fig. 2 are transformed in the curves plotted in Fig. 9. They show a significant size-scale effect, much more evident than in Mode I problems [13].
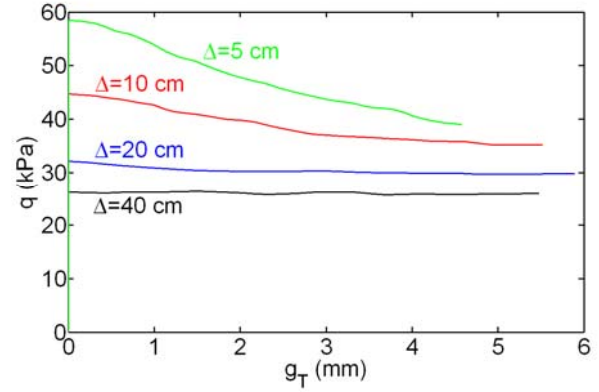

Figure 9: Inelastic post-peak branches obtained from Fig. 2, depending on the specimen size Δ.

In order to obtain a single size-independent cohesive zone model in Mode II, a proper renormalization of the vertical and horizontal coordinates has to be made. Regarding the shear tractions, the scaling law in Eq. (6) suggests to divide q by Δ^{-d_q}, i.e., plotting the scaling invariant material property q^*. The horizontal coordinates can also be renormalized in a similar way, considering the scaling law typical for the displacements which is inspired by the Cantor set [13], i.e., $g_\mathrm{T} = g_\mathrm{T}^* \Delta^{(1-d_g)}$. In this case, the fractal exponent d_g can range from 0 to 0.61, considering the equality relating the sum of the fractal exponents for the strength, the strain and the fracture energy (refer to [13] for more details about the description of the fractal domains).

For the present problem, the best dimensionless representation with the minimum scatter between the curves is obtained for $d_g = 0$, which leads to $g_\mathrm{T}^* = g_\mathrm{T}/\Delta$. The collapse of the curves in Fig. 10 shows that the post-peak branch of the different experimental shear tests can be effectively modelled according to a single scale-invariant Mode II cohesive zone model.
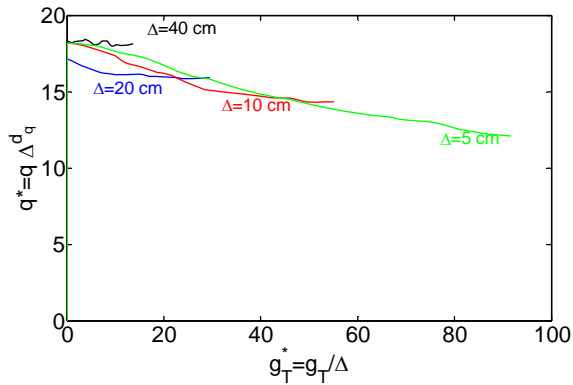
Figure 10: Scale-invariant Mode II cohesive zone model. The various curves correspond to different specimen sizes Δ.

5 CONCLUSIONS

In this work, the fundamental problem of shear transfer between rough surfaces has been analyzed in reference to the existing experimental results available in the literature. Shear tests on rock-rock joints, concrete-concrete interfaces, and concrete-soil foundations present several common aspects. In particular, the pre-peak response of the shear traction vs. sliding displacement curve is highly nonlinear, due to progressive sliding of micro-contacts. After the achievement of the shear strength, the post-peak branch presents softening and plastic plateau, when steel bolts are not included. Finally, the shear strength exhibits a strong size-scale effect, as also typically observed in previous studies regarding Mode I problems [15-17].

In order to interpret both regimes, a hybrid formulation based on contact mechanics for the pre-peak stage and on nonlinear fracture mechanics for the post-peak one has been proposed. This modelling strategy is consistent with the physics of the phenomenon, since the pre-peak response is mainly related to the progressive slippage of micro-contacts, whereas the post-peak behaviour is governed by cohesion originated by asperity interlocking and frictional effects. As a result, we have been able to predict with a reasonable accuracy the pre-peak regime and the related size-scale effects, proposing the simple Eq. (5) and an algorithm easy to use for the simulation of shear tests from the knowledge of the normal contact stiffness. Regarding the post-

peak branches, a single scale-invariant Mode II cohesive zone model has been proposed. This methodology is expected to have an impact in the design formulae for the estimation of the shear strength of cold joints and it overcomes all the main disadvantages of the purely numerical elasto-plastic approach proposed so far in the literature.

ACKNOWLEDGEMENTS

REFERENCES

[1] Randl, N. and Wicke, M., 2000. Schubübertragung zwischen Alt- und Neubeton. *Beton und Stahlbetonbau* **95**: 461-473.

[2] Cottone, A. and Giambanco, G., 2009. Minimum bond length and size effects in FRP–substrate bonded joints. *Engng. Fract. Mech.* **76**:1957-1976.

[3] Bandis, S., Lumsden, A.C. and Barton N.R., 1981. Experimental studies of scale effects on the shear behaviour of rock joints. *Int. J. Rock Mech. Min. Sci. & Geomech. Abstr.* **18**:1-21.

[4] Reul, O., 2000. In-situ-Messungen und numerische Studien zum Tragverhalten der kombinierten Pfahl-Plattengründung, *Tech. Report 53*, Institut und Versuchsanstalt für Geotechnik, TU Darmstadt, Darmstadt, Germany.

[5] Červenka, J., Chandra Kishen, J.M., and Saouma, V.E., 1998. Mixed mode fracture of cementitious bimaterial interfaces; part II: numerical simulation. *Engng. Fract. Mech.* **60**:95-107.

[6] Carpinteri, A. and Paggi, M., 2005. Size-scale effects on the friction coefficient. *Int. J. Sol. and Struct.* 42:2901-2910.

[7] Carpinteri, A. and Paggi, M., 2008. Size-scale effects on strength, friction and fracture energy of faults: a unified interpretation according to fractal geometry. *Rock Mechanics and Rock Engineering* **41**:735-746.

[8] Carpinteri, A. and Paggi, M., 2009. A fractal interpretation of size-scale effects on strength, friction and fracture energy of faults. *Chaos, Solitons and Fractals* **39**:540-546.

[9] Borri-Brunetto, M., Chiaia, B. and Ciavarella, M., 2001. Incipient sliding of rough surfaces in contact: a multiscale numerical analysis. *Comp. Meth. Appl. Mech. Engng.* **190**:6053-6073.

[10] Borri-Brunetto, M., Carpinteri, A., Invernizzi, S. and Paggi, M., 2006. Micro-slip of rough surfaces under cyclic tangential loading, In: P. Wriggers, U. Nackenhorst (Eds.), *Analysis and Simulation of Contact Problems*, Lecture Notes in Applied and Computational Mechanics **27**:333-340, Springer-Verlag, Berlin.

[11] Zavarise, G., Borri-Brunetto, M. and Paggi, M., 2004. On the reliability of microscopical contact models. *Wear* **257**: 229-245.

[12] Paggi, M. and Barber, J.R., 2011. Contact conductance of rough surfaces composed of modified RMD patches. *Int. J. Heat and Mass Transfer* **4**:4664-4672.

[13] Carpinteri, A., Chiaia, B. and Cornetti, P. 2002. A scale-invariant cohesive crack model for quasi-brittle materials. *Eng. Fract. Mech.* **69**:207-217.

[14] Carpinteri, A., Corrado, M. and Paggi, M., 2011. An analytical model based on strain localization for the study of size-scale and slenderness effects in uniaxial compression tests. *Strain* **47**:351-362.

[15] Carpinteri, A., 1994. Fractal nature of material microstructure and size effects on apparent mechanical properties. *Mech. Mater.* **18**:89-101.

[16] Carpinteri, A., 1994. Scaling laws and renormalization groups for strength and toughness of disordered materials. *Int. J. Solids Struct.* **31**:291-302.

[17] Carpinteri, A., Gong, B., and Corrado, M. 2011. Hardening cohesive/overlapping zone model for metallic materials: The size-scale independent constitutive law. *Eng. Fract. Mech.* **82**:29-45.